Arteriosclerosis, Thrombosis, and Vascular Biology

Author Disclosures

Nicola Wilck: No disclosures

Mandy Fechner: No disclosures

Henryk Dreger: No disclosures

Bernd Hewing: No disclosures

Aimara Arias: No disclosures

Silke Meiners: No disclosures

Gert Baumann: No disclosures

Verena Stangl: No disclosures

Karl Stangl: No disclosures

Antje Ludwig: No disclosures

Attenuation of early atherogenesis in LDL receptor deficient mice by proteasome inhibition

Wilck: Proteasome inhibition attenuates atherogenesis

Nicola Wilck[1] (MD), Mandy Fechner[1] (DVM), Henryk Dreger[1] (MD), Bernd Hewing[1] (MD), Aimara Arias[1], Silke Meiners[2] (PhD), Gert Baumann[1] (MD), Verena Stangl[1] (MD), Karl Stangl[1] (MD), Antje Ludwig[1] (PhD)

[1]Medizinische Klinik für Kardiologie und Angiologie, Charité–Universitätsmedizin Berlin, Campus Mitte, Berlin, Germany, [2]Comprehensive Pneumology Center, Ludwig-Maximilians-Universität, Universitätsklinikum Grosshadern und Helmholtz Zentrum München, Munich, Germany

Correspondence to:

Antje Ludwig

Medizinische Klinik für Kardiologie und Angiologie

Charité-Universitätsmedizin Berlin Campus Mitte

Charitéplatz 1

D-10117 Berlin, Germany

Phone: [+49 30] 450 513 286

Fax: [+49 30] 450 513 941

Email: antje.ludwig@charite.de

Word count of body: 5409

Word count of abstract: 197

Total number of figures and tables: 6

Abstract

Objective: Low and non-toxic proteasome inhibition has anti-inflammatory, anti-proliferative and anti-oxidative effects on vascular cells *in vitro* and *in vivo*. We hypothesized that low-dose inhibition of the proteasome could provide anti-atherogenic protection. The present study investigated the effect of low-dose proteasome inhibition on early lesion formation in LDL-receptor-deficient (LDLR-/-) mice fed a Western-type diet.

Methods and Results: Male LDLR-/- mice, 10 weeks old, were fed a Western-type diet for 6 weeks with intraperitoneal injections of bortezomib or solvent. Bortezomib was injected at a dose of 50 µg/kg body weight. Cholesterol plasma levels were not affected by bortezomib treatment. *En face* Oil Red O staining of aortae and aortic root cryosections demonstrated significant reduction of atherosclerotic lesion coverage in bortezomib-treated animals. Bortezomib significantly reduced vascular cellular adhesion molecule-1 expression and macrophage infiltration as shown by histological analysis. Bortezomib treatment resulted in a significant reduction of superoxide content, lipid peroxidation and protein oxidation products, serum levels of monocyte chemoattractant protein-1 and interleukin-6. Gene expression microarray analysis showed that expressional changes induced by Western-type diet were attenuated by treatment with low-dose bortezomib.

Conclusions: Low-dose proteasome inhibition exerts anti-oxidative and anti-inflammatory effects and attenuates development of atherosclerotic lesions in LDLR-/- mice.

Key words: atherosclerosis, proteasome, oxidative stress, inflammation

Atherosclerosis is a vascular disease associated with chronic inflammation and oxidative stress. The pathophysiological process of plaque formation involves early endothelial dysfunction due to increased levels of endogenous reactive oxygen species (ROS). As a consequence, the bioavailability of nitric oxide and endothelium-dependent vasodilation are reduced. Those alterations promote increased expression of adhesion molecules (e.g. VCAM-1) in endothelial cells followed by cell surface adhesion of circulating leukocytes and their subsequent migration into the vessel wall. Accumulating mononuclear cells release a variety of cytokines and chemokines, such as MCP-1, guiding more inflammatory cells to the site and thereby driving the progression of the atherosclerotic lesion. Ultimately, smooth muscle cells, immune cells and cholesterol-loaded macrophages accumulate and contribute to the deposition of extracellular matrix, lipids and necrotic debris within the developing atherosclerotic plaque which in turn results in narrowing of the vessel diameter [1-2].

The ubiquitin-proteasome system (UPS) is the major pathway for intracellular protein degradation in eukaryotic cells [3]. Beyond its function to degrade dysfunctional proteins, the UPS is involved in various regulatory processes including transcription, apoptosis, and cell cycle. For example, the UPS activates important transcription factors, such as pro-inflammatory nuclear factor-κB (NF-κB) and the oxidative-stress-related nuclear erythroid 2-related factor 2 (Nrf2) [4].

An excellent review of studies concerning the UPS in atherosclerosis by Herrmann et al. showed the progress made in recent years towards understanding the role of the UPS in plaque formation [5]. A dual role of the UPS was postulated: First, the UPS contributes to lesion formation by mediating the inflammatory response; second, that it may have a protective role by eliminating dysfunctional proteins. Accordingly, differential effects of proteasome inhibition (PI) were suggested, depending on the stage of atherosclerotic disease [5].

Cellular responses to proteasome inhibition (PI) are divergent and range from induction of apoptosis to protection from cell death [6]. Cytotoxic properties of PI were recognized early and led to clinical application of the proteasome inhibitor bortezomib in treatment of multiple myeloma [7].

Furthermore, proteasome inhibitors have also been identified as potent anti-inflammatory drugs in a number of acute and chronic inflammatory animal models [6].

We proposed the concept of proteasome inhibitors acting as poisons or remedies. That is: seemingly contradictory effects of PI may be the result of different dosages used, or could depend on a cell- or tissue-specific susceptibility to inhibitors [6]. Depending on the resulting degree of inhibition, PI could thus mediate either cytotoxic or beneficial effects.

Treatment with low doses of proteasome inhibitors exerted favorable anti-inflammatory and anti-oxidative effects in vascular cells [8-12]. Moreover, low-dose PI was shown to enhance eNOS expression and activity, improved endothelial function [13] and prevented TNF-α-induced vascular dysfunction by reducing superoxide production and decreasing endothelin-1 levels in rat aortic rings [14]. We have recently shown that low-dose PI down-regulates TNF-α-induced expression of VCAM-1 in endothelial cells and in a hypertensive rat model, which suggests that low-dose PI suppresses inflammatory cell adhesion in atherogenesis [11]. Taken together, low-dose PI effectively modulates factors and processes particularly important during early-stage atherosclerosis.

On the basis of these considerations, we hypothesized that low-dose proteasome inhibition provides anti-atherogenic protection and could delay the onset of atherosclerosis. We investigated early lesion formation in Western-type diet-fed LDL-receptor-deficient mice that represent a well-established model of hypercholesterolemia-induced atherosclerosis. Animals were treated with low doses of the boronate-type proteasome inhibitor bortezomib. The observed attenuation of atherosclerotic lesion formation supports our hypothesis that low-dose PI provides anti-atherogenic protection *in vivo*.

Methods

Materials

Unless otherwise specified, all reagents and media were purchased from Sigma Chemicals, Germany. Bortezomib was kindly provided by Millenium Pharmaceuticals.

Animal experiments

Animal experiments were approved by the local authority (Landesamt für Gesundheit und Soziales, Berlin) and were performed according to institutional guidelines.

Dosing studies were performed by employing Ub^{G76V}-GFP-1 mice (Charles River, Germany), which express the green fluorescence protein (GFP) as transgene from a chicken β-actin promoter [15]. Ub^{G76V}-GFP-1 males were bred with C57BL/6 females for maintenance. Heterozygous Ub^{G76V}-GFP1 adult males were injected once with the indicated doses of bortezomib or saline, 24 h before they were sacrificed by collection of whole blood (by puncture of the retroorbital vein plexus) under isoflurane anesthesia. Following perfusion with PBS, heart and aortae were snap-frozen in liquid nitrogen for storage at -80°C.

Male 10-week-old LDLR-/- mice (B6.129S7-*Ldlr*^{tm1Her}/J; JAX Mice, Boston) were divided into three body weight and serum cholesterol matched groups. Mice of the WD group were fed a high fat diet for 6 weeks *ad libitum* (Western-type diet containing 21% butterfat, 17% casein, 0.21% cholesterol; Ssniff, Soest, Germany) and received intraperitoneal saline injections. Mice of the WD+Bor group received the same Western-type diet for 6 weeks and intraperitoneal injections of bortezomib (50 µg/kg body weight) twice weekly. The CD group received a low fat control diet. General condition and body weight were monitored.

Mice were fasted for two hours, anesthetized in an isoflurane-loaded box and euthanized. After perfusion with PBS, heart and aortae were dissected under a stereomicroscope (Leica), snap-frozen in

liquid nitrogen and stored at -80°C or fixed in formalin. Livers were snap-frozen immediately for analysis of proteasomal activity.

Measurement of proteasomal activity

Measurement of proteasomal activity in liver lysates was performed as described previously [11] (see online supplement).

Staining and analysis of atherosclerotic lesions

For *en face* aortic lesion analysis, thoracic aortae were stained with Oil Red O. Lesion area in the aortic arch was calculated as percentage of total aortic arch area. Cryosections of aortic roots were stained with Oil Red O and counterstained with hemalaun. Analysis was performed under standardized conditions using Zeiss Axiovision Software. Results were calculated as the percentage of lipid-stained area of total vessel area (see online supplement for details of staining, imaging and quantification).

Immunohistochemistry

Immunohistochemistry of acetone-fixed 5 µm aortic root cryosections was performed using anti-VCAM-1 (Pharmingen) and anti-Mac-2 (Cedarlane laboratories). Following hemalaun counterstain sections were digitally photographed under standardized conditions using Zeiss AxioCam MrC and analyzed using Zeiss AxioVision software (see online supplement for details of staining protocols).

***In situ* superoxide detection**

DHE staining was used to assess vascular superoxide production (see online supplement).

Measurement of serum lipids and lipid peroxidation products

Plasma total cholesterol and triglyceride concentrations were measured by colorimetric enzymatic assay (CHOL-PAP, and TG GPO-PAP, Roche-Diagnostics, Mannheim, Germany). HDL-cholesterol

concentration was separated by the phosphotungstate-magnesium precipitation technique, followed by measurement as for total cholesterol.

Lipid hydroperoxides were determined in mouse serum by measurement of the formation of thiobarbituric-acid reactive substances (TBARS), as described previously [11, 16] (see online supplement).

Serum levels of MCP-1 and IL-6

Serum levels of mouse soluble MCP-1 and mouse IL-6 were measured by Mouse CCL2/JE/MCP-1 or IL-6 Quantikine ELISA Kit (R&D Systems, Inc., Minneapolis, MN, USA) according to the manufacturer's protocol.

Western blot

Tissue lysis and Western blot analysis were performed according to established protocols [11] (see online supplement).

Quantitative real-time RT-PCR

RNA isolation and real-time RT-PCR were performed as previously described [11] (see online supplement).

Gene expression microarray and bioinformatical analysis

Agilent Whole Mouse Genome Oligo Microarrays of pooled aortic lysates were performed and analyzed as described in detail in the online supplement. In brief, RNA was isolated using TRIzol reagent, quality-checked via the Agilent 2100 Bioanalyzer platform and amplified. RNA expression was analyzed in two independent experiments. For each experiment, RNA from 4 animals per group (CD, WD, WD+Bor) was pooled. 1.65 μg Cy3-labeled fragmented cRNA in hybridization buffer was hybridized overnight (17 hours, 65°C) to Agilent Whole MouseGenome Oligo Microarrays (4x44K). Fluorescence signals of the

hybridized Agilent Microarrays were detected using Agilent's Microarray Scanner System (Agilent Technologies, Palo Alto, USA). The Agilent Feature Extraction Software (FES) was used to read out and process the microarray image files.

For determination of differential gene expression FES derived output data files were further analyzed using the Rosetta Resolver® gene expression data analysis system (Rosetta Biosoftware, Seattle, USA). In order to receive unbiased information on the functional pattern among genes regulated by Western-type diet the software tool Ontologizer v2.1 (Computational Biology Group, Institute for Medical Genetics and Human Genetics, Charité–Universitaetsmedizin Berlin, Germany, http://compbio.charite.de/index.php/ontologizer2.html) was used to analyze microarray data.

Analysis of vasoreactivity

Analysis of vasoreactivity of mouse aortic rings was performed according to established protocols [8,13,14] (see online supplement).

Statistical analysis

Data are presented as mean ± SEM. Comparisons between groups were made using Mann-Whitney or Student's t test, or one-way ANOVA plus Tukey post hoc test (SPSS v18.0) as appropriate. $P < 0.05$ was considered significant.

Gene expression microarray data was analyzed using the Rosetta Resolver® gene expression data analysis system (Rosetta Biosoftware, Seattle, USA). A *p*-value was calculated for every –fold change using the Rosetta Resolver error model. All genes with expression ratios < 0.5 and > 2 and a $p < 0.01$ were selected to generate the tables of significantly regulated genes.

Results

Dose adjustment for non-toxic proteasome inhibition

In order to define a low and non-toxic, but effective dose of the proteasome inhibitor bortezomib, we performed experiments with Ub^{G76V}-GFP-1 reporter mice. Following administration of 500 µg/kg BW bortezomib, we observed an accumulation of Ub^{G76V}-GFP in cell lysates of aortae as well as in heart tissue as measured in Western blots, upon probing with anti-GFP antibodies (Figure 1). Western blot analyses of the same cell lysates with anti-ubiquitin antibodies revealed that 50 µg/kg bortezomib was sufficient to cause an increase in the level of ubiquitin conjugates, albeit less pronounced than in lysates of animals treated with 500 µg/kg BW bortezomib (Figure 1). Application of 25 µg/kg BW bortezomib had no measurable effects. Therefore, 50 µg/kg BW bortezomib, which is well below the toxic dosage of 100 µg/kg BW established for monkeys and rodents [7,17], represents a moderate but effective dose for PI in the cardiovascular system and was used in the current study.

Male LDLR-/- mice, 10 weeks of age, were fed a Western-type diet for 6 weeks and received either intraperitoneal bortezomib injections (WD+Bor; n = 12), or saline injections (WD; n = 12) twice weekly for 6 weeks. Mice kept on a normal low fat control diet served as control group (CD; n = 6). Bortezomib treatment (WD+Bor) resulted in a 32.8 % inhibition of the chymotrypsin-like activity compared to WD animals, as measured in liver lysates 24 hours after the final injection (Table 1) and was well tolerated by the mice. Body weight was similar in all groups at time of harvesting. No abnormalities in livers, kidneys, or blood counts were detected following bortezomib treatment (data not shown). No signs of elevated apoptosis were observed in vessels of WD+Bor mice (Supplementary Figure S1). Western diet caused significant elevation of plasma cholesterol and triglyceride concentrations. Bortezomib treatment had no effect on plasma cholesterol or triglyceride levels (Table 1).

Low-dose bortezomib attenuates early atherosclerotic lesion formation

LDLR-/- mice fed a Western-type diet for 6 weeks developed early lesions almost exclusively in the aortic arch area and the aortic root, whereas aortas of age-matched CD LDLR-/- had no detectable lesions, as shown by *en face* and cross-sectional analysis. *En face* analysis of atherosclerotic lesions in the aortic arch (Figure 2A) revealed a significant reduction of lesion area in the WD+Bor compared to the WD group (0.52 ± 0.08 versus 1.29 ± 0.20 % of total aortic area; $p = 0.007$). Likewise, Oil Red O stained area in the aortic root (Figure 2B) was significantly reduced in WD+Bor animals compared to WD mice (5.67 ± 0.59 versus 19.36 ± 2.46 % of total vessel area; $p < 0.001$).

Low-dose bortezomib provides anti-inflammatory protection in LDLR-/- mice

VCAM-1 expression was examined in aortic root cryosections of LDLR-/- mice. Bortezomib treatment significantly decreased VCAM-1 staining (2.85 ± 0.42 versus 6.55 ± 1.15 %; $p < 0.038$; Figure 2C).

Compared to CD mice, serum levels of monocyte chemoattractant protein-1 (MCP-1) were significantly increased in WD mice. Bortezomib significantly lowered MCP-1 serum levels of WD mice (39.72 ± 3.07 versus 53.49 ± 2.85 pg/ml; $p = 0.004$, Figure 3A). Mac-2 positive macrophage content in aortic root cryosections was decreased in WD+Bor compared to WD animals (2.61 ± 0.25 versus 9.10 ± 1.41 %; $p < 0.001$; Figure 2D). Serum levels of interleukin 6 (IL-6) were found to be strongly increased in WD compared to CD mice. Remarkably, in WD+Bor mice, IL-6 levels were maintained nearly at the level of CD mice (Figure 3B).

Low-dose bortezomib exerts anti-oxidative effects in LDLR-/- mice

We performed *in situ* detection of superoxide production by fluorescence microscopy in sections of the ascending aorta. Dihydroethidium (DHE) fluorescence revealed marked reduction of superoxide release in WD+Bor compared to WD mice (196.99 ± 36.97 versus 368.26 ± 46.52 arbitrary units; $p < 0.02$; Figure 2E). Serum levels of lipid peroxidation products measured as TBARS were significantly decreased (4.37 ± 0.24 versus 7.58 ± 0.53 µmol/l; $p < 0.001$; Figure 4A) in WD+Bor mice as compared to WD mice. Stable

vascular oxidation products were examined in aortic lysates. Bortezomib treatment caused reduction of protein oxidation as measured by detection of carbonyl groups using OxyBlot compared to WD and even to CD animals (Figure 4B).

We previously described transcriptional down-regulation of NADPH oxidase subunit Nox4 expression by low-dose PI in endothelial cells [8]. In line with this finding, Real-Time RT-PCR using aortic RNA showed a reduction of Nox4 mRNA expression in WD+Bor mice compared to WD mice (Figure 4C).

Low-dose bortezomib attenuates WD-induced changes in gene expression

Expression microarray analysis identified approximately 3900 genes that were regulated by more than twofold in WD mice compared to CD animals. Interestingly, only about 1500 of these genes were regulated by more than twofold in mice that received bortezomib in addition to Western-type diet.

Bioinformatic analysis revealed that genes associated with the GO terms 'cell communication' (GO:0007154), 'oxidation reduction' (GO:0055114), and 'generation of precursor metabolites and energy' (GO:0006091) were significantly overrepresented ($p < 0.001$) among regulated genes in Western-type diet mice (Supplementary Figure S2). Only less than half of this subset of genes was regulated by more than twofold in mice that received bortezomib in addition to Western-type diet.

Similar results were obtained when we focussed on a selection of genes which have been shown to play a role in atherosclerosis (Figure 5). Here, bortezomib again markedly suppressed gene expression changes induced by Western-type diet, including MCP-1, VCAM-1 and IL-6, confirming our above described observations.

Taken together, WD-induced regulation of genes was attenuated by bortezomib treatment, leading to an expressional pattern in WD+Bor animals approaching that of CD animals. Surprisingly, no significant change in expression of catalytic and non-catalytic proteasomal subunits was in detected in all groups. Ubiquitin C-terminal hydroxylase L1 (Uchl1), a deubiquitinating hydrolase that has been

associated with suppression of neointima formation and suppression of NF-κB activation [18], shows a favorable regulation in WD+Bor compared to WD mice.

Vasoreactivity of aortic rings is preserved

Determination of vasoreactivity is of particular interest, since data concerning the effect of PI on vasoreactivity are controversial [19]. To assess possible modulation of vasoreactivity by bortezomib treatment, we evaluated endothelium-dependent and endothelium-independent vasodilation of isolated aortic rings by acetylcholine and sodium nitroprusside, respectively. As shown in Supplementary Figure S3A vasoreactivity in response to acetylcholine was equally potent in the WD and WD+Bor groups. Likewise, endothelium-independent vasodilation following sodium nitroprusside application was similar in both groups (Supplementary Figure S3B). Aortic rings tested did not show atherosclerotic lesions as shown for the aortic arch, which is consistent with the early-stage atherosclerosis in the current study.

Discussion

In the present study we have shown an anti-atherosclerotic effect of low-dose treatment with the proteasome inhibitor bortezomib in LDLR-/- mice. Early atherosclerotic lesion formation was significantly attenuated by bortezomib treatment, without changing plasma cholesterol levels. This was attributed to a marked reduction of oxidative stress and vascular inflammation.

An important issue was the adjustment of PI dosage such that detectable modulation of proteasome activity could be achieved without inducing toxicity, even during long-term treatment. Since no such studies have been conducted in mice regarding the cardiovascular system in this context, we made use of the Ub^{G76V}-GFP-1 transgenic reporter mouse [15]. Degradation of the Ub^{G76V}-GFP fusion protein is readily detectable and is sensitive to PI [20]. A level of 500 µg/kg BW bortezomib was highly effective for PI in this system: however, this dose is toxic [7]. A considerably lower non-toxic dose (50 µg/kg BW) still led to detectable accumulation of polyubiquitinated proteins, thereby demonstrating at least partial

inhibition of proteasomal activity. This was further verified by observation of a reduced chymotrypsin-like proteasome activity in liver tissue following 6-week treatment of mice with this low dose of bortezomib. Bortezomib treatment at this dosage for 6 weeks did not lead to apoptosis in the vasculature. According to a previous report on hypertensive rats [11], partial PI at this dosage is also not toxic, while exerting potent anti-oxidative and anti-inflammatory effects. Anti-atherogenic effects of low-dose bortezomib treatment can therefore be attributed to partial inhibition of the proteasome.

There is substantial evidence from cell culture experiments supporting anti-inflammatory and anti-oxidative properties of low-dose PI [8-12,21]. One mechanism mediating the anti-oxidative effects of low-dose PI in cardiovascular cells is stabilization of oxidative stress related transcription factor Nrf2 [9,21]. In line with these previous *in vitro* observations, we found definite anti-oxidative effects of low-dose bortezomib treatment in hypercholesterolemic LDLR-/- mice in the present study. Serum content of lipid peroxidation products, which was markedly increased in hypercholesterolemic LDLR-/- mice compared to control diet-fed LDLR-/- mice, was significantly decreased by bortezomib treatment. Similar data were obtained on stable protein oxidation and lipid peroxidation products. Moreover, vascular superoxide production, measured by DHE fluorescence, was decreased by bortezomib, which is similar to results previously observed in hypertensive rats treated with bortezomib [11]. NADPH oxidases are considered a major source of ROS in the vasculature [22]. Gene expression microarray analysis revealed that of all Nox isoforms, only Nox4 was significantly regulated in our model, which was confirmed by Real-Time RT-PCR. This is of particular interest, since previous cell culture experiments identified Nox4 as susceptible to proteasome inhibition [8]. The underlying mechanism for Nox4 down-regulation by low-dose PI is unknown. Above all, gene expression microarray analysis indicates that certainly multiple proteins contribute to the anti-oxidative effect of low-dose bortezomib.

Since oxidative stress is a key element of endothelial dysfunction, we examined the vasoreactivity of isolated aortic rings. Unlike previously published data on coronary circulation [23], endothelium-dependent vasorelaxation of aortic rings was not affected by PI in the present study. However, beneficial anti-oxidative effects of low-dose bortezomib treatment in LDR-/- mice did not translate into improved

endothelium-dependent vasorelaxation. Taking recent studies into consideration, the effect of PI on endothelial function remains puzzling [19]. Recent reports suggested that chronic inhibition of the UPS mediates dysfunctional effects in coronary arteries of hypercholesterolemic pigs [23], while vascular function in the renal circulation of the same model was shown to be improved [24]. Thus, in addition to possible inhibitor-specific and dose-dependent effects of PI on endothelial function, variable responses of different vascular beds to PI are conceivable. It is debatable whether data shown here are of minor relevance to vasomotor function of the thoracic aorta, which represents a conductance rather than a resistance vessel. Vasoreactivity of resistance vessels was not tested in the current study, but appears to be more suitable to illustrate the functional consequence of the endothelium-protective effects induced by low-dose bortezomib treatment in early atherosclerosis.

Anti-oxidative properties of low-dose PI have recently been shown to be the underlying mechanism for inhibition of TNF-α-induced monocyte adhesion to endothelial cells and attenuation of hypertension-induced VCAM-1 expression in hypertensive rats, representing an alternative anti-inflammatory pathway beyond inhibition of NF-κB translocation by PI [11]. The present study confirms anti-inflammatory effects in a widely accepted mouse model of atherosclerosis. We observed a PI-induced reduction of central pro-inflammatory mediators MCP-1 and VCAM-1. It appears that down-regulation of MCP-1 and VCAM-1 is of functional relevance, since it leads to decreased subendothelial macrophage content in PI-treated hypercholesterolemic LDLR-/- mice. Moreover, the WD-induced increase of IL-6 plasma levels was almost completely blocked by treatment with low-dose bortezomib. Since leukocytes are certainly the primary source of MCP-1 and IL-6 production [25], anti-inflammatory capacities of low-dose PI are evidently not limited to resident vascular cells, but may also involve migrating inflammatory cells. Of note, attenuation of MCP-1 secretion was also observed in a previous *in vitro* study investigating the reduced secretion of MCP-1 and RANTES in dendritic cells exposed to non-toxic doses of bortezomib [26]. Interestingly, another potentially protective effect by PI was demonstrated in a very recent study: PI increased the expression of functional ATP-binding cassette transporters A1 (ABCA1) and ABCG1, thereby increasing the cholesterol efflux from macrophages and promoting overall reverse cholesterol

transport in vivo [27]. Short-term treatment of BL6 with bortezomib resulted in enhancement of ABCA1 und decrease of SRB1, but was not accompanied by increase in HDL cholesterol. Chronic bortezomib treatment of hypercholesterinemic mice in our study did also not induce changes in HDL cholesterol and total cholesterol. However, we cannot exclude that beneficial effects on reverse cholesterol transport contribute to the anti-atherogenic effect of bortezomib observed in our study.

Indeed, anti-oxidative and anti-inflammatory effects of low-dose bortezomib treatment resulted in significant reduction of early lesion size in hypercholesterolemic LDLR-/- mice, as shown by *en face* analysis of the aortic arch and by cross-sectional analysis of aortic root cryosections.

Earlier reports [23] suggest that chronic inhibition of the UPS aggravates atherosclerosis in coronary arteries of hypercholesterolemic pigs by causing oxidative stress, thereby promoting endothelial dysfunction and vascular inflammation This apparent contradiction to our results, which show beneficial actions of partial non-apoptotic PI in the vascular system, may be explained by considering dose-dependent and organ-specific effects of PI, as extensively discussed over the past two years [5,6,28,29]. While pronounced proteasome inhibition appears to stimulate ROS production and pro-inflammatory processes in blood vessels [23], inhibitor treatment at moderate doses provides anti-oxidative and thereby anti-inflammatory protection, as shown here *in vivo* and in earlier *in vitro* and *in vivo* models [11].

Limitations:

The present study provides the first *in vivo* demonstration of the beneficial action of low-dose PI on very early lesion formation, which supports the concept of PI to counteract initiation of atherosclerosis. No conclusion can be drawn regarding the effect of PI in late-stage atherosclerosis. A recent study indicates that PI on developed lesions promotes features of a 'rupture-prone' plaque phenotype in ApoE-/- mice without affecting the plaque size [30]. Since there is evidence for a dual role of the UPS in the course of atherogenesis [5], a yet undefined time frame for beneficial effects of PI may exist.

Currently, comparability to other studies is limited, since inhibitor concentrations vary among different studies. Future studies should take into account the pronounced dose-dependency of PI-mediated effects

as well as possible organ-specific effects, to collectively explore the potential and the limitations of utilization of low-dose PI in atherosclerosis.

Investigation of the vasoreactivity of resistance arteries could clarify whether the currently described unchanged vasoreactivity in the thoracic aorta is modulated in smaller vessels.

Although there have been promising findings regarding atherosclerosis and prevention of restenosis [31], therapeutic application of proteasome inhibitors in the cardiovascular system requires further profound and systematic investigations.

In conclusion, low-dose PI attenuates early atherosclerosis. These findings further highlight the involvement of the UPS in the pathophysiology of atherosclerosis. Specifically, the suspected role of the UPS in initiation of the disease by oxidative stress and inflammatory processes has been verified *in vivo*.

Acknowledgments

We are grateful for the excellent assistance of Susanne Metzkow and Anke Stach. We thank Dr. Stewart Russell for helpful criticism.

Sources of Funding

This work was supported by a grant from the foundation Deutsche Stiftung für Herzforschung [F/02/05] to KS and AL.

Disclosures

None.

References

1. Ross R. Atherosclerosis: an inflammatory disease. *N Engl J Med.* 1999;340:115-126.

2. Glass CK, Witztum JL. Atherosclerosis. The road ahead. *Cell* 2001;104:503–516.

3. Goldberg AL. Protein degradation and protection against misfolded or damaged proteins. *Nature* 2003;426:895–899.

4. McMahon M, Itoh K, Yamamoto M, Hayes JD. Keap1-dependent proteasomal degradation of transcription factor Nrf2 contributes to the negative regulation of antioxidant response element-driven gene expression. *J Biol Chem.* 2003;278:21592–21600.

5. Herrmann J, Lerman LO, Lerman A. On to the road to degradation: atherosclerosis and the proteasome. *Cardiovasc Res*. 2010;85:291-302.

6. Meiners S, Ludwig A, Stangl V, Stangl K. Proteasome inhibitors: poisons and remedies. *Med Res Rev*. 2008;28:309-327.

7. Bross PF, Kane R, Farrell AT, Abraham S, Benson K, Brower ME, Bradley S, Gobburu JV, Goheer A, Lee SL, Leighton J, Liang CY, Lostritto RT, McGuinn WD, Morse DE, Rahman A, Rosario LA, Verbois SL, Williams G, Wang YC, Pazdur R. Approval summary for bortezomib for injection in the treatment of multiple myeloma. *Clin Cancer Res.* 2004;10:3954-3964.

8. Meiners S, Ludwig A, Lorenz M, Dreger H, Baumann G, Stangl V, Stangl K. Nontoxic proteasome inhibition activates a protective antioxidant defense response in endothelial cells. *Free Radic Biol Med.* 2006;40:2232–2241.

9. Dreger H, Westphal K, Wilck N, Baumann G, Stangl V, Stangl K, Meiners S. Protection of vascular cells from oxidative stress by proteasome inhibition depends on Nrf2. *Cardiovasc Res*. 2010;85:395-403.

10. Bieler S, Meiners S, Stangl V, Pohl T, Stangl K. Comprehensive proteomic and transcriptomic analysis reveals early induction of a protective anti-oxidative stress response by low-dose proteasome inhibition. *Proteomics* 2009;12:3257-3267.

11. Ludwig A, Fechner M, Wilck N, Meiners S, Grimbo N, Baumann G, Stangl V, Stangl K. Potent anti-inflammatory effects of low-dose proteasome inhibition in the vascular system. *J Mol Med*. 2009;8:793-802.

12. Westphal K, Stangl V, Fähling M, Dreger H, Weller A, Baumann G, Stangl K, Meiners S. Human-specific induction of glutathione peroxidase-3 by proteasome inhibition in cardiovascular cells. *Free Radic Biol Med*. 2009;47:1652-1660.

13. Stangl V, Lorenz M, Meiners S, Ludwig A, Bartsch C, Moobed M, Vietzke A, Kinkel HT, Baumann G, Stangl K. Long-term up-regulation of eNOS and improvement of endothelial function by inhibition of the ubiquitin-proteasome pathway. *FASEB J.* 2004;18:272-279.

14. Lorenz M, Wilck N, Meiners S, Ludwig A, Baumann G, Stangl K, Stangl V. Proteasome inhibition prevents experimentally-induced endothelial dysfunction. *Life Sci.* 2009;84:929-934.

15. Lindsten K, Menéndez-Benito V, Masucci MG, Dantuma NP. A transgenic mouse model of the ubiquitin/proteasome system. *Nat Biotechnol*. 2003;21:897-902.

16. Wong SH, Knight JA, Hopfer SM, Zaharia O, Leach CN Jr, Sunderman FW Jr. Lipoperoxides in plasma as measured by liquid-chromatographic separation of malondialdehyde-thiobarbituric acid adduct. *Clin Chem.*1987;33:214-220.

17. Cavaletti G, Gilardini A, Canta A, Rigamonti L, Rodriguez-Menendez V, Ceresa C, Marmiroli P, Bossi M, Oggioni N, D'Incalci M, De Coster R. Bortezomib-induced peripheral neurotoxicity: a neurophysiological and pathological study in the rat. *Exp Neurol.* 2007;204:317-325.

18. Takami Y, Nakagami H, Morishita R, Katsuya T, Cui TX, Ichikawa T, Saito Y, Hayashi H, Kikuchi Y, Nishikawa T, Baba Y, Yasuda O, Rakugi H, Ogihara T, Kaneda Y. Ubiquitin carboxyl-terminal hydrolase L1, a novel deubiquitinating enzyme in the vasculature, attenuates NF-kappaB activation. *Arterioscler Thromb Vasc Biol*. 2007;10:2184-2190.

19. Stangl K, Stangl V. The ubiquitin proteasome pathway and endothelial (dys)function. *Cardiovasc Res*. 2010;85:281-290.

20. Dantuma NP, Lindsten K, Glas R, Jellne M, Masucci MG. Short-lived green fluorescent proteins for quantifying ubiquitin/proteasome-dependent proteolysis in living cells. *Nat Biotechnol.* 2000;18:538-543.

21. Dreger H, Westphal K, Weller A, Baumann G, Stangl V, Meiners S, Stangl K.Nrf2-dependent upregulation of antioxidative enzymes: a novel pathway for proteasome inhibitor-mediated cardioprotection. *Cardiovasc Res*. 2009;83:354-361.

22. Griendling KK, Sorescu D, Ushio-Fukai M. NAD(P)H oxidase: role in cardiovascular biology and disease. *Circ Res.* 2000;86:494–501.

23. Herrmann J, Saguner AM, Versari D, Peterson TE, Chade A, Olson M, Lerman LO, Lerman A. Chronic proteasome inhibition contributes to coronary atherosclerosis. *Circ Res.* 2007;101:865-874.

24. Chade AR, Herrmann J, Zhu X, Krier JD, Lerman A, Lerman LO. Effects of proteasome inhibition on the kidney in experimental hypercholesterolemia. *J Am Soc Nephrol.* 2005;4:1005-1012.

25. Tedgui A, Mallat Z. Cytokines in atherosclerosis: pathogenic and regulatory pathways. *Physiol Rev*. 2006;86:515-581.

26. Nencioni A, Schwarzenberg K, Brauer KM, Schmidt SM, Ballestrero A, Grünebach F, Brossart P. Proteasome inhibitor bortezomib modulates TLR4-induced dendritic cell activation. *Blood*. 2006;108:551-558.

27. Ogura M, Ayaori M, Terao Y, Hisada T, Iizuka M, Takiguchi S, Uto-Kondo H, Yakushiji E, Nakaya K, Sasaki M, Komatsu T, Ozasa H, Ohsuzu F, Ikewaki K. Proteasomal Inhibition Promotes ATP-Binding Cassette Transporter A1 (ABCA1) and ABCG1 Expression and Cholesterol Efflux From Macrophages In Vitro and In Vivo. *Arterioscler Thromb Vasc Biol*. 2011;9:1980-1987.

28. Fukai T. Targeting proteasome worsens atherosclerosis. *Circ Res*. 2007;101:859-861.

29. Ludwig A, Meiners S. Targeting of the proteasome worsens atherosclerosis? *Circ Res*. 2008;102:e37.

30. Van Herck JL, De Meyer GR, Martinet W, Bult H, Vrints CJ, Herman AG. Proteasome inhibitor bortezomib promotes a rupture-prone plaque phenotype in ApoE-deficient mice. *Basic Res Cardiol*. 2010;105:39-50.

31. Meiners S, Laule M, Rother W, Guenther C, Prauka I, Muschick P, Baumann G, Kloetzel PM, Stangl K. Ubiquitin-proteasome pathway as a new target for the prevention of restenosis. *Circulation* 2002;105:483-489.

Figure legends

Figure 1. Injection of 50 µg/kg BW bortezomib leads to partial proteasome inhibition. Western blot analysis of Ub^{G76V}GFP reporter protein and ubiquitin conjugates in aorta and myocardium of wildtype (WT) and Ub^{G76V}GFP-1 transgenic mice, 24 hours after intraperitoneal injection of bortezomib. 50 µg/kg BW bortezomib is the first dose leading to accumulation of ubiquitin conjugates, whereas accumulation of the Ub^{G76V}GFP fusion protein is still not detectable, which indicates partial inhibition of proteasomal activity. In contrast, injection of 500 µg/kg BW bortezomib leads to pronounced proteasomal inhibition with increased accumulation of ubiquitin conjugates and accumulation of the Ub^{G76V}GFP reporter protein. Amidoblack staining as loading control (LC).

Figure 2. Bortezomib significantly reduces atherosclerotic lesion size, VCAM-1 expression, macrophage infiltration and vascular superoxide production. Male LDLR-/- mice were fed a Western diet with intraperitoneal injection of saline (WD) or bortezomib (WD+Bor) for 6 weeks. **A,** *En face* Oil Red O staining of thoracic aorta shows reduction of early atherosclerotic lesions in bortezomib-treated animals. *p = 0.007, n = 8 per group. **B,** Oil Red O cryosections of the aortic root reveal reduction of atherosclerotic lesions in bortezomib-treated animals.*p < 0.001, n = 8 per group. **C,** Reduction of VCAM-1 expression in bortezomib-treated animals. *p = 0.038; n = 8. **D,** Mac-2 staining of aortic root cryosections reveals reduction of macrophage content in bortezomib-treated animals. *p < 0.001, n = 8. **E,** Bortezomib (WD+Bor) reduces DHE fluorescence compared to solvent-treated animals (WD). DHE fluorescence in red, autofluorescence in green. *p < 0.02, n = 6-7.

Figure 3. Serum parameters confirm anti-inflammatory effects of low-dose proteasome inhibition. **A**, Elevated MCP-1 serum levels in WD mice are significantly decreased by bortezomib (WD+Bor). n = 12 per group; #p < 0.001 vs. CD; *p = 0.004 vs. WD. **B**, Western-diet-induced elevation of IL-6 serum levels is significantly diminished by bortezomib. n = 12; #p = 0.01 vs. CD, *p = 0.007 vs. WD. *CD* control-diet, *WD* Western diet, *Bor* proteasome inhibitor bortezomib.

Figure 4. Bortezomib reduces lipid peroxidation, vascular protein oxidation and Nox4 mRNA expression. A, Serum levels of TBARS as a marker for lipid peroxidation. Increase in WD (compared to CD) is significantly lowered by bortezomib (WD+Bor). n = 11-12 per group; #p < 0.001 vs. CD; *p < 0.001 vs. WD. **B,** Western diet-induced increase of oxidized proteins in aortae of LDLR-/- mice is reduced by bortezomib. Pooled lysates of thoracic aorta from 6 animals. Representative OxyBlot. **C**, Bortezomib treatment (WD+Bor) reduces mRNA expression of Nox4 NADPH oxidase subunit in aortae of LDLR-/- mice. Quantitative Real-Time RT-PCR of mRNA isolated from whole aorta. n=8 per group; #p < 0.05 vs. CD; *p < 0.05 vs. WD. *CD* control-diet, *WD* Western diet, *Bor* proteasome inhibitor Bortezomib, *LC* Amidoblack staining as loading control.

Figure 5. Bortezomib suppresses changes in expression of atherosclerosis-relevant genes induced by Western-type diet, as shown by gene expression analysis. Heat map shows significantly regulated genes (p < 0.01) summarized in subgroups, expressed as x-fold alteration of expression levels of bortezomib-treated animals (WD+Bor) and Western-type diet fed animals (WD) versus control diet fed mice (CD). RNA taken from whole aortae of four animals per group. Mean values from two different replicates using two independent RNA pools.

Table 1. Body weight, cholesterol and triglycerides concentrations and proteasomal activities in LDLR-/- mice

	CD (n=6)	**WD (n=12)**	**WD + Bor (n=12)**
Body weight, g	28.7 ± 0.6	30.8 ± 0.7	30.2 ± 0.6
Total cholesterol, mg/dl	244 ± 11	998 ± 72	1002 ± 52
HDL-cholesterol	71.3±2.1	83.7±8.5	87.2±6.8
Triglycerides, mg/dl	80 ± 10	902 ± 93	834 ± 91
Proteasomal activity in liver lysates, RFU	1242 ± 84.39	1194 ± 163 (100 %)	801 ± 56 ***** (67.2 %)

CD control-diet, *WD* Western diet, *Bor* proteasome inhibitor bortezomib. *p<0.05

Figure 1

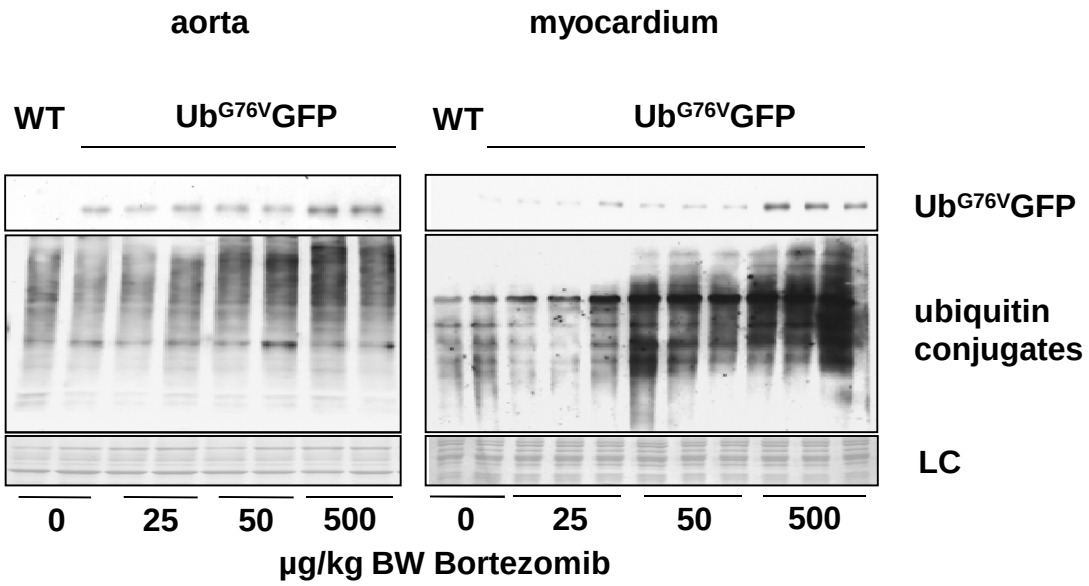

Figure 2

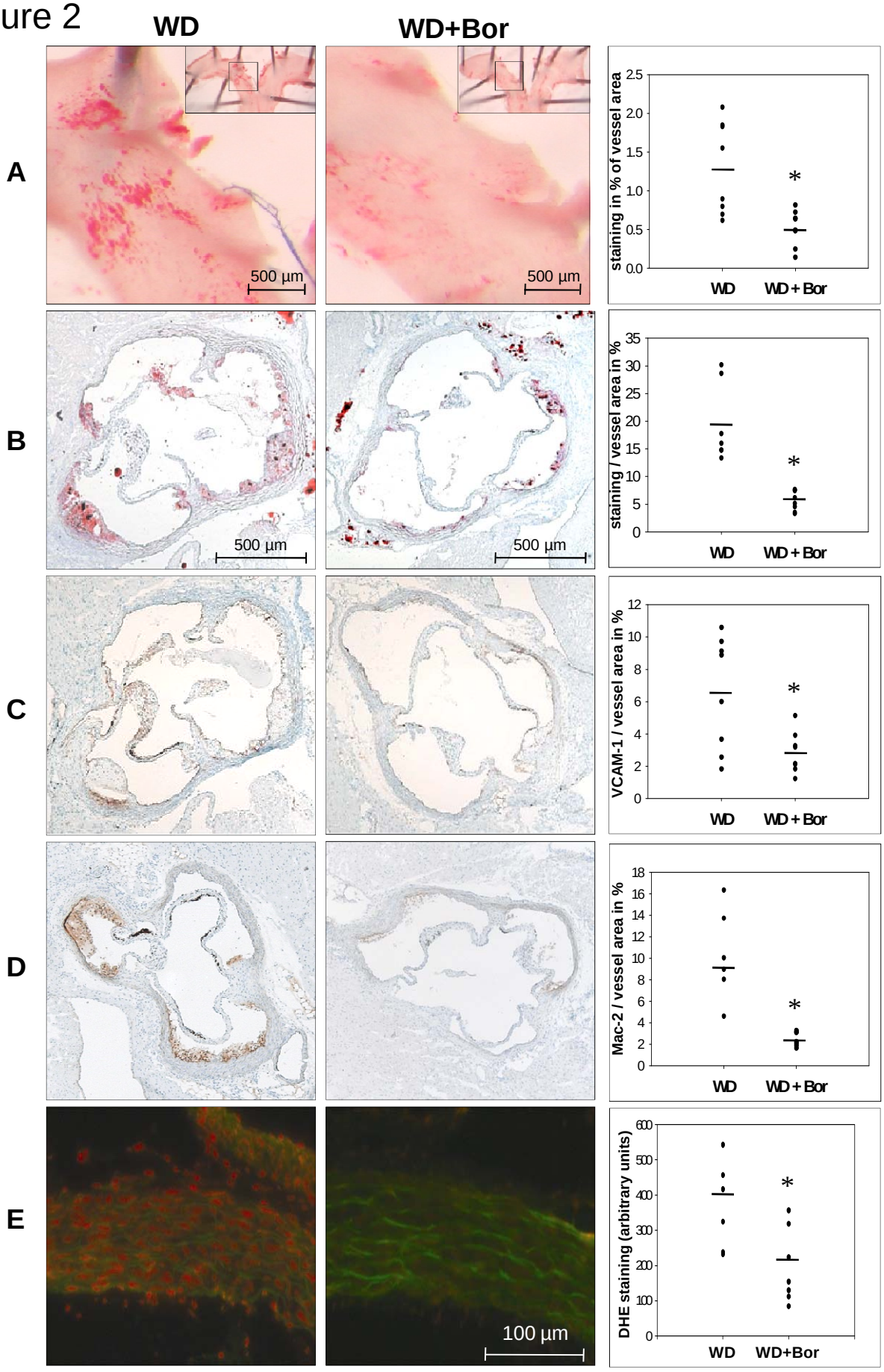

Figure 3

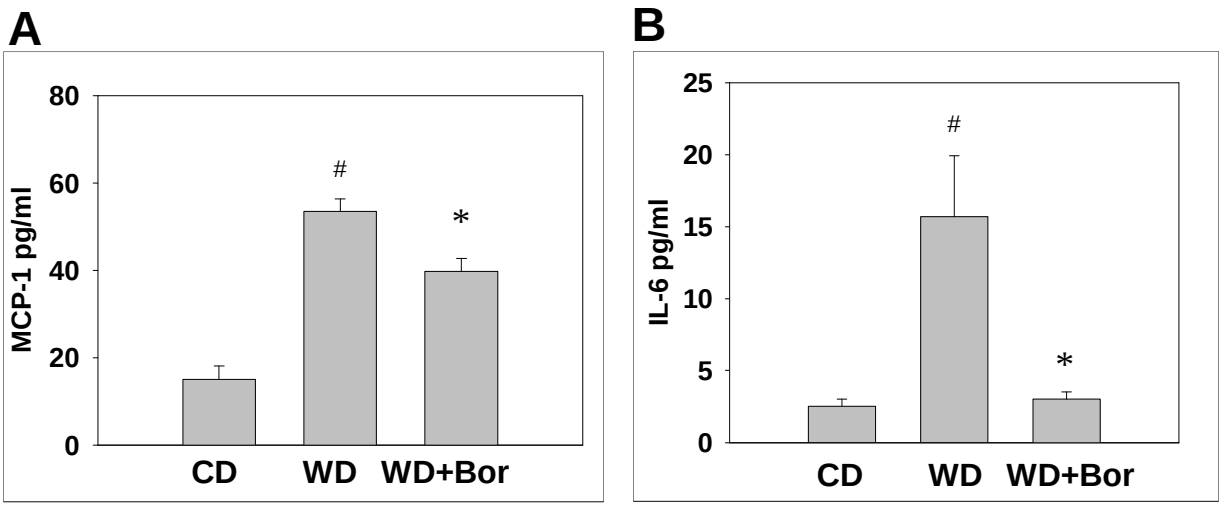

Figure 4

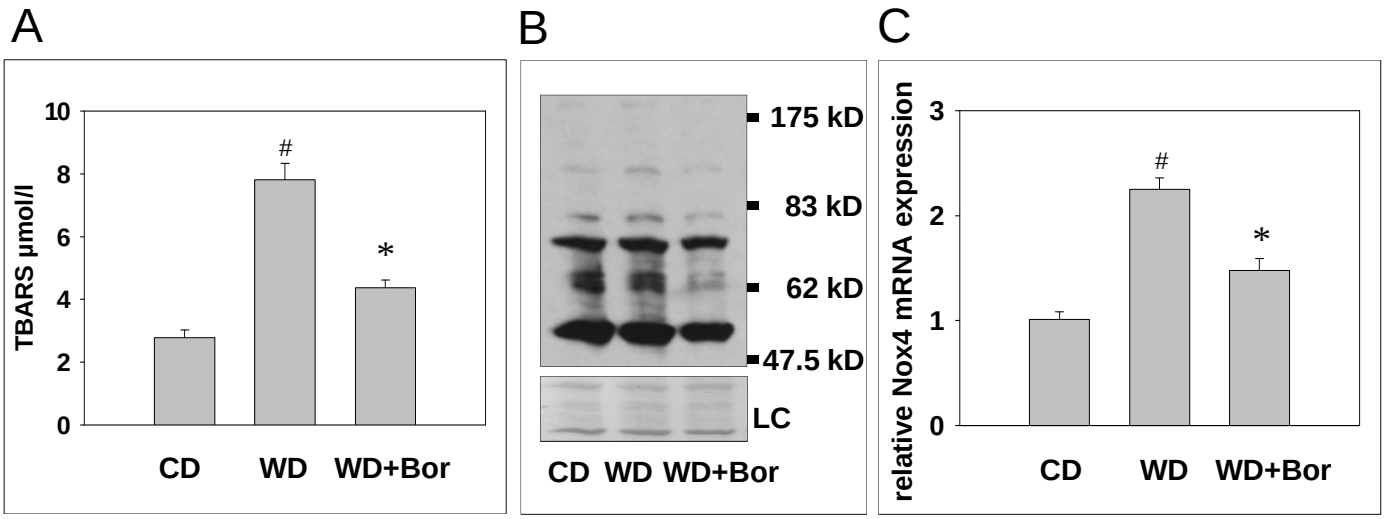

Figure 5